Limits to the experimental detection of nonlinear synchrony

Paul So,[1,*] Ernest Barreto,[1] Krešimir Josić,[2] Evelyn Sander,[3] and Steven J. Schiff[4]
[1]*Department of Physics and Astronomy and the Krasnow Institute for Advanced Study, George Mason University, Fairfax, Virginia 22030*
[2]*Department of Mathematics, Boston University, Boston, Massachusetts 02215*
[3]*Department of Mathematical Sciences, George Mason University, Fairfax, Virginia 22030*
[4]*Department of Psychology and the Krasnow Institute for Advanced Study, George Mason University, Fairfax, Virginia 22030*
(Received 6 August 2001; revised manuscript received 16 January 2002; published 9 April 2002)

Chaos synchronization is often characterized by the existence of a continuous function between the states of the components. However, in coupled systems without inherent symmetries, the synchronization set can be extremely complicated. We describe and illustrate three typical complications that can arise, and we discuss how existing methods for detecting synchronization will be hampered by the presence of these features.

DOI: 10.1103/PhysRevE.65.046225 PACS number(s): 05.45.−a, 87.10.+e, 87.19.La

Since the surprising discovery that chaotic systems can synchronize [1,2], many different kinds of nonlinear synchrony have been considered in the literature [3]. In this paper, we focus on the concept of generalized synchronization (GS) [2,4,5] of coupled *nonidentical* systems. GS is a useful concept in the analysis of physical and biological systems comprised of multiple components. Emergent features within such systems are characterized by coherent behavior among their components; for example, the perception of sensory input may correspond to synchronized activity between layers of the cortex [6]. The experimental detection and classification of such synchronized states is challenging, and recently attempts have been made to broaden the concept of GS with special emphasis on applications in biology [7,8].

Geometrically, GS is characterized by the existence of a continuous map $\phi: X \to Y$ between the phase spaces X, Y of two systems. This map associates a state of the first system with a state of the second in such a way that graph (ϕ) is invariant and attracting under the evolution of the coupled system [9]. In the presence of symmetries, graph (ϕ) frequently has a simple structure.

In drive-response systems GS is equivalent to *asymptotic stability* [5] if the driving system is *invertible* and has a compact attractor. A system is asymptotically stable if, for any two initial conditions $(\mathbf{x}_0, \mathbf{y}_0'), (\mathbf{x}_0, \mathbf{y}_0'') \in X \times Y$ which share the same initial drive state, $\lim_{n\to\infty} ||\mathbf{y}_n(\mathbf{y}_0', \mathbf{x}_0) - \mathbf{y}_n(\mathbf{y}_0'', \mathbf{x}_0)|| = 0$, where $\mathbf{y}_n(\cdot,\cdot)$ represents iteration of the response system under the full dynamics. As a consequence, a common drive can enslave multiple copies of the response [10]; this is similar to the idea of "reliable response" in the generation of neuronal signals [11,12].

The detection of GS in practice relies strongly on the *continuity* of ϕ [4,7,13], and in general also requires a certain degree of smoothness of ϕ. Tight clusters of points in X need to be mapped to similarly clustered points in Y under ϕ. The existence of GS has been demonstrated in both physical [14] and biological systems [7] using this concept. However, variations and mismatches are typical for coupled systems in nature and, as we show in this paper, coupled systems lacking intrinsic symmetries can exhibit synchronization sets with very complicated structures. In particular, for coupled invertible systems, the synchronization set can become nondifferentiable by "wrinkling," developing cusps, and in the more severe case of noninvertible systems, it can become "smeared." If "smearing" occurs, the function ϕ is in general replaced by a *multivalued* relation, even though the response is still asymptotically stable. These features may severely hamper the detection of nonlinear synchrony. The aim of this work is to comprehensively address the intrinsic *limits* to detecting nonlinear synchrony.

We propose a categorization of the structures which arise in such synchronization states, and link these structures to universal features of the component's dynamics. While we expect the situation to be similar in bidirectionally coupled systems, we consider a drive-response system as our model to simplify the analysis:

$$\mathbf{x}_{n+1} = \mathbf{f}(\mathbf{x}_n),$$

$$\mathbf{y}_{n+1} = \mathbf{g}(\mathbf{x}_n, \mathbf{y}_n, c). \tag{1}$$

The drive $\mathbf{x} \in X$ and the response $\mathbf{y} \in Y$ are state vectors and both $\mathbf{f}$ and $\mathbf{g}$ are smooth or piecewise smooth maps. The parameter c characterizes the interaction strength. For systems described by ordinary differential equations, a Poincaré section can be used to reduce the system to a discrete map.

The first type of nontrivial structure has been studied in [15,16], and we include it for completeness. Following [15] we use the following choices for the maps in (1): $\mathbf{x} = (u, v)$, y is a scalar, and

$$u_{n+1} = \begin{cases} \lambda u_n, & v_n < \alpha \\ \lambda + (1-\lambda) u_n, & v_n \geqslant \alpha, \end{cases}$$

$$v_{n+1} = \begin{cases} v_n/\alpha, & v_n < \alpha \\ (v_n - \alpha)/(1-\alpha), & v_n \geqslant \alpha \end{cases} \tag{2}$$

$$y_{n+1} = c y_n + \cos 2\pi u_{n+1},$$

*Electronic address: http://complex.gmu.edu

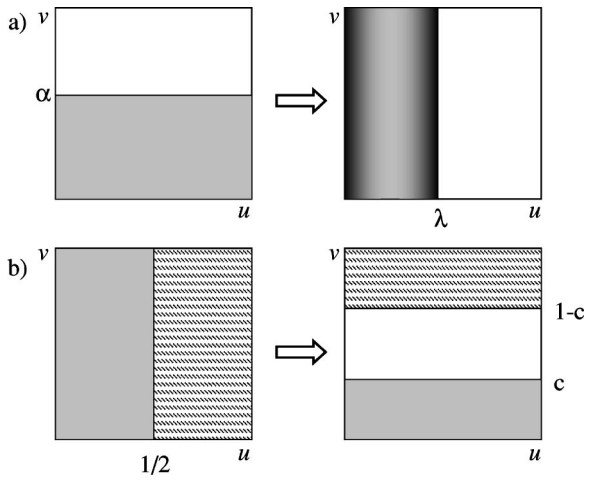

FIG. 1. (a) Generalized Baker's map. Gray scale indicates the contraction rate in Eq. (3). (b) ''Thin'' Baker's map.

with $0<\lambda<1$ and $0<\alpha<1$. The drive is the generalized Baker's map taking the unit square to two nonoverlapping rectangles as shown in Fig. 1(a). The response y is a filter of the drive's variable u with c controlling the contraction rate. If $|c|<1$, the response is asymptotically stable for all $\mathbf{x}$. As pointed out in [15,16], the synchronization set is typically nondifferentiable if the average contraction within the drive is larger than the contraction in the response. In particular, if h_d is the least negative past-history Lyapunov exponent [17] of the drive and h_r is the contracting past-history Lyapunov exponent in the transverse direction (with $|h_r|<|h_d|$), then ϕ is generally nondifferentiable with a Hölder exponent [18] given by $|h_r/h_d|<1$ [15]. Since the generalized Baker's map has uniform measure in v, the synchronization set can be visualized in the uy plane. Graphs demonstrating both the differentiable and nondifferentiable case are given in Figs. 2(a) and 2(b), respectively. We call this development of nondifferentiability ''wrinkling.''

The wrinkling of the synchronization manifold is a *local* feature, and the smoothness in the vicinity of a single orbit depends on the ratio of the exponents h_r and h_d along this orbit. Thus there typically exist invariant sets embedded in the synchronization set on which ϕ has differing degrees of regularity [19]. As we will demonstrate below, there are situations in which nondifferentiability on these ''smaller'' sets may become important.

In an experimental situation, the loss of smoothness of ϕ can mask the underlying coherence in the coupled system. Consider the following numerical test based on the definition of continuity. After transients die out, pick a point $(\mathbf{x},\mathbf{y})$ on the attractor and a small number δ, and iterate the full system until the $\mathbf{x}$ component of the trajectory lands in the ball $B[\mathbf{x},\delta]$ a large number of times. Keep track of these points, and denote by $\epsilon_{\max}$ the largest distance between their corresponding $\mathbf{y}$ components. If ϕ is differentiable, then typically $\epsilon_{\max}\rightarrow 0$ linearly as $\delta\rightarrow 0$. This is not the case when $|h_d|>|h_r|=|\ln c|$; instead, $\epsilon_{\max}\rightarrow 0$ sublinearly as δ decreases, and the slope of the function $\epsilon_{\max}(\delta,\mathbf{x})$ corresponds roughly to the Hölder exponent of ϕ at $\mathbf{x}$. An ensemble of these scaling curves can be studied for a collection of random chosen $\mathbf{x}$. When $|h_d|<|\ln c|$, ϕ is smooth almost everywhere and $\epsilon_{\max}$ depends linearly on δ as shown in Fig. 3(a). When $|h_d|>|\ln c|$, $\epsilon_{\max}$ decreases sublinearly with δ [Fig. 3(b)] and ϕ is *only* Hölder continuous.

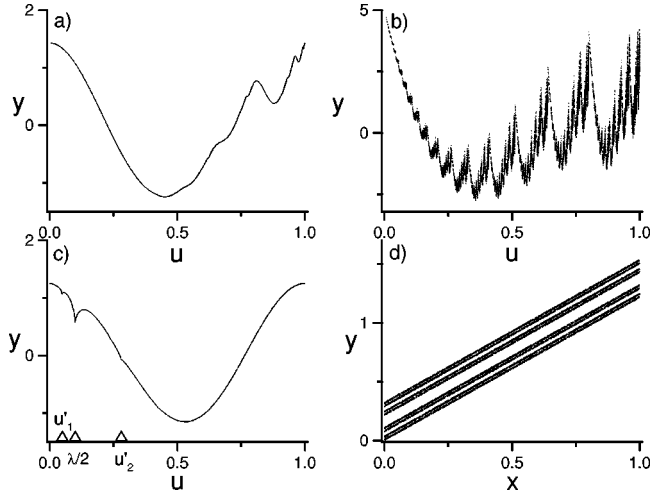

FIG. 2. Complicated structures in synchronization sets: (a) smooth case with $|h_d|<|h_r|(h_r=\ln 0.3)$; (b) wrinkled case with Hölder exponent given by $|h_r/h_d|<1(h_r=\ln 0.8)$. In both (a) and (b), $\lambda=0.8$ and $\alpha=0.7$. This choice gives $h_d=-0.64$. (c) Cusped case with $\lambda=0.2$, $\alpha=0.3$, and $c=0.2$. $h_d=-0.90$ in this case. The cusps occur at the forward iterates of the critical point at $u=1/2$, and the largest three (indicated by markers) are located at $u=0.1$, 0.0488, and 0.28. (d) Smeared case with $c=0.35$.

This $\epsilon_{\max}-\delta$ test is the idea behind most GS detection methods. Of course, finite data and experimental noise may adversely affect the procedure, but we emphasize that the presence of wrinkling, which is an intrinsic feature of the dynamics, may significantly hinder the detection of generalized synchrony. As a result, it may not be possible to reliably predict the response from the drive even if the drive can be measured with high accuracy.

The second type of structure that can develop within the synchronization set results from critical points in the drive's

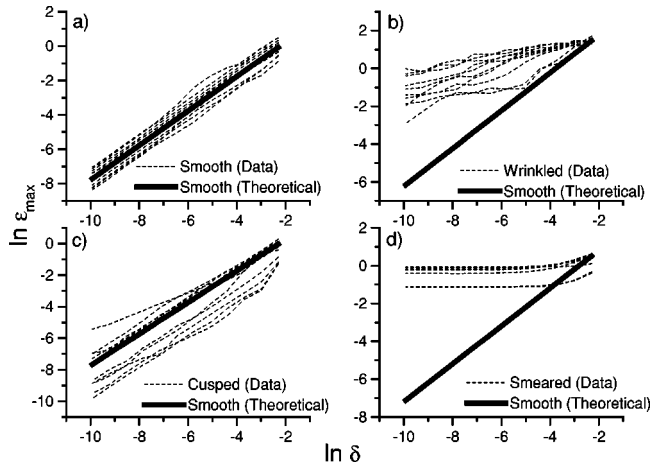

FIG. 3. Result of the $\epsilon_{\max}-\delta$ test: (a) smooth, (b) wrinkled, (c) cusped, and (d) smeared. The thick solid line is the expected linear scaling if ϕ is differentiable. Parameters are the same as in Fig. 2.

attractor. At a critical point, the Jacobian matrix of **f** is singular, so that within a neighborhood of these points we can expect the existence of orbits in X along which the contraction is large compared to the magnitude of h_r. As a result graph (ϕ) will typically not be differentiable near the critical points. Although the local mechanism resulting in the nondifferentiability of ϕ is similar to wrinkling, the structure of the synchronization set and the resulting limits on synchrony detection are different. We demonstrate this difference using the following modification of the drive in Eq. (2):

$$u_{n+1}=\begin{cases}4\lambda[(u_n-1/2)^3+1/8], & v_n<\alpha\\ \lambda+(1-\lambda)u_n, & v_n\geqslant\alpha,\end{cases}$$

$$v_{n+1}=\begin{cases}v_n/\alpha, & v_n<\alpha\\ (v_n-\alpha)/(1-\alpha), & v_n\geqslant\alpha,\end{cases} \tag{3}$$

where the response y is as in Eq. (2). In this example, the drive maps the unit square onto two nonoverlapping rectangles [see Fig. 1(a)] as before. However, the contraction rate in the u direction is no longer uniform. The linear map $(u_{n+1}=\lambda u_n)$ is replaced by a cubic map $(u_{n+1}=4\lambda[(u_n-1/2)^3+1/8])$, which is invertible and has a critical point at $u=1/2$. The dependence of the contraction rate on u is indicated by the gray scale in Fig. 1(a). Along the line $u=1/2$ the contraction rate is infinite. As in the previous example, the synchronization set can be visualized as a graph in the uy plane (see Fig. 2(c)). The parameters are chosen so that for almost every orbit the past-history Lyapunov exponent h_d in the drive is less than the normal contraction rate $h_r=\ln c$. Since $|h_r/h_d|>1$ for almost every orbit, the synchronization set is smooth almost everywhere. However, graph ϕ is not completely smooth since ''cusps'' are formed at and near the critical point and its iterates. The biggest cusp appears at $u=\lambda/2$, which is the forward image of $u=1/2$. The Hölder exponent at $u=\lambda/2$ is zero regardless of h_r, and the shape of graph (ϕ) at $u=\lambda/2$ is consistent with this prediction.

This graph also contains an infinite number of smaller cusps. Since the cubic map in Eq. (3) maps the critical line $u=\lambda/2$ to two lines at $u_1'=\lambda^2/2(\lambda^2-3\lambda+3)$ and $u_2'=\lambda/2(3-\lambda)$ [marked by triangles in Fig. 2(c)], two more cusps appear at these locations, and further cusps appear under subsequent iterates of the critical line [20].

Although graph (ϕ) is not smooth in either the cusped or the wrinkled case, its global structure in the two cases is different. The wrinkles in the first example depend on the strength of the contraction rate in the **y** direction, and for $c<\min(\lambda,1-\lambda)$, graph (ϕ) is differentiable everywhere. On the other hand, the critical line in the cusped case is an intrinsic feature of the drive, and the Hölder exponent at $u=\lambda/2$ and its forward iterates will vanish for all values of the contraction rate $h_r=\ln c$. In this case graph (ϕ) is nondifferentiable for *all* values of c. Second, the nondifferentiability in the wrinkled case typically has a stronger effect on the detectibility of GS. Since wrinkling occurs almost everywhere when $|h_r/h_d|<1$, the $\epsilon_{\max}-\delta$ test fails at almost every point in the drive. In the cusped case, the cusps occur at and near the critical line $u=1/2$, and decrease in size at its forward iterates due to contraction. Thus they do not affect the $\epsilon_{\max}-\delta$ test as severely. The difference between the two cases can be described more quantitatively using wavelet analysis [19].

Figure 3(c) shows an ensemble of scaling curves for the $\epsilon_{\max}-\delta$ test in the cusped case. $\epsilon_{\max}$ depends linearly on δ at most points **x** up to the resolution of the data, as expected. Occasionally a scaling curve has a slope less than one indicating the lack of regularity of ϕ for a value of u near one of the ''cusps.''

The third type of structure which may hinder the detection of GS is the development of striations in the synchronization set when the drive is *noninvertible*. Although many systems can be modeled by ordinary differential equations and are thus assumed to have time-invertible dynamics, there are important physical and biological examples in which noninvertibility plays an important role. Traditional descriptions of population dynamics in biology utilize noninvertible maps [21]. Models with time delays, for which temporal invertibility is not guaranteed [22], are typical in neuronal processes. Most importantly, the dynamics reconstructed from discrete-time samples of systems with strong dissipation is frequently best approximated by noninvertible maps [23].

Due to noninvertibility, a typical state of the drive will have a whole tree of possible histories, and recurrences in the drive may thus occur along different routes. Each such route provides a different driving signal, and this occurs independently of the coupling strength c. Therefore, even if the response is asymptotically stable, for almost all points in the drive there typically correspond a Cantor set of points in the response: one for each drive history, [see Fig. 2(d)] [8] thus resulting in a striated structure for the synchronization set. A different and less severe form of multivalued synchronization where the drive and response are related by an $1:m$ ratio is reported in [24,25].

The striated structure of this synchronization set is best understood in a two-dimensional piecewise linear version of system (1)

$$x_{n+1}=f(x_n)=\begin{cases}2x_n, & x_n<0.5\\ 2(x_n-0.5), & x_n\geqslant 0.5,\end{cases} \tag{4}$$

$$y_{n+1}=g(x_n,y_n,c)=cy_n+x_{n+1},$$

where f is noninvertible with two preimages for each x_{n+1}. For $|c|<1$, the synchronization set is asymptotically stable. Figure 2(d) is a typical picture of the synchronization set and consists of a Cantor set of lines. Although the topology of the synchronization set for a more general noninvertible drive-response system will be different, the structure illustrated by this example is a typical feature.

The structure of this synchronization set can be understood using a linear transformation of the full (x,y) system by a matrix $\mathbf{T}(c)$, $(\tilde{x}\,\tilde{y})^{\mathrm{T}}=\mathbf{T}(x\,y)^{\mathrm{T}}$, where

$$\mathbf{T}(c)=\begin{pmatrix}1 & 0\\ -2(1-c)/c & (2-c)(1-c)/c\end{pmatrix}. \tag{5}$$

In the new coordinates, system (4) becomes the ''thin'' Baker's map given by

$$\tilde{x}_{n+1}=\begin{cases}2\tilde{x}_n, & \tilde{x}_n<0.5\\ 2(\tilde{x}_n-0.5), & \tilde{x}_n\geqslant 0.5,\end{cases}$$

$$\tilde{y}_{n+1}=\begin{cases}c\tilde{y}_n, & \tilde{x}_n<0.5\\ c\tilde{y}_n+(1-c), & \tilde{x}_n\geqslant 0.5.\end{cases} \tag{6}$$

Under one iteration, the two halves of the unit square are mapped into two rectangles as before [see Fig. 1(b)]. For $c<0.5$, this map is area contracting with a rate given by $2c$. After n iterations, the original unit square is mapped to 2^n horizontal strips of height c^n, and the limiting set of this process is a Cantor set of lines. The attracting set of the original map (4) [see Fig. 2(d)] is the image of this Cantor set of lines under the transformation $\mathbf{T}^{-1}(c)$.

Figure 3(d) demonstrates the effect of these striated structures on the $\epsilon_{\max}-\delta$ test. Since the synchronization set is a graph of a one-to-∞ relation, $\epsilon_{\max}>0$ for all values of $\mathbf{x}$ and δ. Once $\epsilon_{\max}$ reaches the thickness of the striated set, it no longer decreases as a function of δ. This can be seen in the saturated scaling curves in Fig. 3(d). Consequently, the ability to predict the state of the response system from the state of the drive will be severely limited, and the situation cannot be improved by increasing the precision of the measurements. The striated structure and the resulting limits on GS detection are consequences of the noninvertibility of the drive.

In summary, for coupled systems without symmetries, the synchronization set can develop very complicated structure. We have described and illustrated three generic features which can arise in the synchronization set from the inherent dynamics; these are likely to coexist in more general systems [26,27]. The presence of these structures implies that the dynamical coherence of the coupled system will be difficult to detect from experimental data, even if the system is asymptotically stable. Current detection methods relying on continuity may very well fail and the presumed mutual predictability between synchronized components might become practically useless. Experimental noise might also hamper the detection of nonlinear synchrony, but the dynamical limitations detailed here are intrinsic to a given system and they cannot be improved by a more careful experiment or by noise reduction techniques.

This work was supported by the NSF-IBN 9727739 and NIH 2R01MH50006 (P.S. and S.S.), 7K0ZMH01493 (S.S), and 1K25MH01963 (E.B.).

[1] H. Fujisaka and T. Yamada, Prog. Theor. Phys. **69**, 32 (1983); L.M. Pecora and T.L. Carroll, Phys. Rev. Lett. **64**, 821 (1990).
[2] V. Afraimovich, N.N. Verichev, and M.I. Rabinovich, Radiophys. Quantum Electron. **29**, 795 (1986).
[3] M. Rosenblum, A. Pikovsky, and J. Kurths, Phys. Rev. Lett. **76**, 1804 (1996); M.G. Rosenblum, A.S. Pikovsky, and J. Kurths, *ibid.* **78**, 4193 (1997); S. Boccaletti, L.M. Pecora, and A. Pelaez, Phys. Rev. E **63**, 066219 (2001).
[4] N.F. Rulkov, M.M. Sushchik, L.S. Tsimring, and H.D.I. Abarbanel, Phys. Rev. E **51**, 980 (1995).
[5] L. Kocarev and U. Parlitz, Phys. Rev. Lett. **76**, 1816 (1996).
[6] F. Varela, J.P. Lachaux, E. Rodriguez, and J. Martinerie, Nat. Rev. Neurosci. **2**, 229 (2001); E. Rodriguez *et al.*, Nature (London) **397**, 430 (1999); C.M. Gray, Neuron **24**, 31 (1999).
[7] S.J. Schiff *et al.*, Phys. Rev. E **54**, 6708 (1996).
[8] E. Barreto, P. So, B.J. Gluckman, and S.J. Schiff, Phys. Rev. Lett. **84**, 1689 (2000).
[9] A weaker definition of GS given in Ref. [4] requires the existence of a function Φ between *trajectories* of the two components. Most GS detection methods use the definition stated in the text.
[10] H.D.I. Abarbanel, N.F. Rulkov, and M.M. Sushchik, Phys. Rev. E **53**, 4528 (1996).
[11] A system responds reliably to an input if its response is identical each time the input is presented. This was demonstrated in a neuronal system in [12].
[12] H.L. Bryant and J.P. Segundo, J. Physiol. (London) **260**, 279 (1976); Z.F. Mainen and T.J. Sejnowski, Science **268**, 1503 (1995).
[13] L.M. Pecora, T.L. Carroll, and J.F. Heagy, Phys. Rev. E **52**, 3420 (1995); H. D. I. Abarbanel, *Analysis of Observed Chaotic Data* (Springer Verlag, New York, 1996).
[14] L.M. Pecora *et al.*, Chaos **7**, 520 (1997); N.F. Rulkov, *ibid.* **6**, 262 (1996).
[15] B.R. Hunt, E. Ott, and J.A. Yorke, Phys. Rev. E **55**, 4029 (1997).
[16] V. Afraimovich, J.-R. Chazottes, and A. Cordonet, Phys. Lett. A **283**, 109 (2001); K. Josić, Nonlinearity **13**, 1321 (2000); J. Stark, Ergod. Theor. Dyn. Syst. **19**, 155 (1999); L. Kocarev, U. Parlitz, and R. Brown, Phys. Rev. E **61**, 3716 (2000); K. Pyragas, *ibid.* **54**, R4508 (1996).
[17] For a typical point $(\mathbf{x},\mathbf{y})$ in the synchronization set, consider an orbit segment consisting of the T preimages of $(\mathbf{x},\mathbf{y})$ under the dynamics of Eq. (1). We can calculate the finite-time Lyapunov exponents over this orbit emanating from the Tth preimage to the current point $(\mathbf{x},\mathbf{y})$. For $T\rightarrow\infty$, if this spectrum of Lyapunov exponents remains the same for almost all $(\mathbf{x},\mathbf{y})$ with respect to the natural measure, then we call these the past-history Lyapunov exponents of the system.
[18] The Hölder exponent of ϕ at x is $\liminf_{\delta\rightarrow 0}\{\log|\phi(x+\delta)-\phi(x)|/\log|\delta|\}$ if it is less than 1 and equal to 1 if it is larger.
[19] E. Baarreto *et al.* (unpublished).
[20] Cusps also form at periodic orbits sufficiently close to these primary cusps.
[21] R.M. May, Nature (London) **261**, 459 (1976).
[22] H. Steinlein and H.-O. Walther, J. Dyn. Diff. Equations **3**, 325 (1990).
[23] E. Ott, *Chaos in Dynamical Systems* (Cambridge University. Press, New York, 1993); E.N. Lorenz, J. Atmos. Sci. **20**, 130 (1963); R.H. Simoyi, A. Wolf, and H.L. Swinney, Phys. Rev. Lett. **49**, 245 (1982); W.L. Ditto, S.N. Rauseo, and M.L.

Spano, *ibid.* **65**, 3211 (1990); M.R. Guevara, L. Glass, and A. Shrier, Science **214**, 1350 (1981); G. Matsumoto *et al.*, J. Theor. Neurobiol. **3**, 1 (1984).

[24] N.F. Rulkov *et al.*, Phys. Rev. E **64**, 016217 (2001); N.F. Rulkov and C.T. Lewis, *ibid.* **63**, 065 204R (2001).

[25] The mechanism for smearing differs fundamentally from this type of multivalueness. The 1:2 multivalued state shown in [24] results from a bifurcation of the response system as the coupling is lowered, while the presence of smearing results from the intrinsic noninvertibility of the drive and is independent of the strength of the coupling. One should note that the examples in Ref. [24] are not *globally* asymptotically stable. This means that for a given history of the drive, two different initial response states do not necessarily have the same asymptotic state on the m ($m=2$ in this case) branches. In contrast, smearing is more ''synchronized'' in the sense that for a given history of the drive, there is only one unique asymptotic response state despite the unavoidable cantor-like structure of the synchronization set.

[26] Wrinkled and smeared synchronization sets were observed in a coupled electronic circuit experiment [27].

[27] J.C. Chubb, E. Barreto, P. So, and B.J. Gluckman, Int. J. Bifurcation Chaos Appl. Sci. Eng. **11**, 2705 (2001).